Comparison of electromagnetic scattering measurements to simulation for microelectronic structures

David P. Paul[a)]
EMIT Systems, Brookline, Massachusetts 02446

Edward W. Conrad
IBM Microelectronics, Essex Junction, Vermont 05452

Daniel C. Cole[b)] and Eytan Barouch
Department of Manufacturing Engineering, Boston University, 15 St. Mary's Street, Brookline, Massachusetts 02446

(Received 11 February 2002; accepted for publication 7 May 2002)

We present an electromagnetic-based method that enables prediction of microlithographic structures of 100 nm and below, for analyzing manufacturability of next-generation microchip technology in real time, *in situ*. The method is robust, versatile, precise, and fast, and experimentally verified by using both scanning electron microscopy and atomic force microscopy. © *2002 American Institute of Physics.* [DOI: 10.1063/1.1489708]

This letter presents experimental verification of simulation predictions from electromagnetic scattering analysis for typical structures of interest in semiconductor technologies. Measured profiles of these structures using scanning electron microscopy (SEM) and atomic force microscopy (AFM) measurements are compared here with electromagnetic scattering computations. Close agreement is obtained for the entire nanoscale sidewall profile of these line structures. At the end of this letter, we briefly comment on why this is achievable, despite that the detailed structural shapes are well below the incident wavelength. With the use of recently reported advanced algorithm developments,[1] combined with the general method[2] of scatterometry measurements, it appears that practical, rapid, and nondestructive measurements for use in advanced microelectronic and nanoelectronic technologies are attainable for 2D and 3D structures.

The experimental setup used here consisted of an instrument similar to a standard optical microscope, but also containing a polarizer, spectral separator, and a light intensity detector. A broadband source of light was used to illuminate periodic 2D microelectronic structures. Reflected spectral intensity was measured in the visible wavelength range (i.e., 450–800 nm) with 6 nm bandwidth. A 5× objective lens with the smallest possible numerical aperture was used to achieve near-normal incidence. Polarization was achieved with a high-efficiency double-prism polarizer placed in the postocular reflected path. Measurements could be taken for two sets of polarization at each wavelength, namely, for light in a transverse electric (TE) mode, where the electric field was oriented in a direction perpendicular to the direction of the grating lines, and for transverse magnetic (TM) field orientation, where the electric field is oriented parallel to the grating lines.

Figure 1 shows scatterometry measurements for a 1000 nm periodic line/space structure created using Shipley 3008 photoresist on bare silicon. Superimposed on the intensity versus wavelength plots is the modeled photoresist profile that was used to generate the modeled intensity versus wavelength curve. As can be seen, close agreement was obtained between the measured and simulated intensity profiles. We have carried out a detailed study where this same structure is examined under considerably different focus-exposure conditions, thereby generating lines both narrower and broader in width, as well as different heights. In each case, agreement very similar in character to that shown here was obtained between the measured and simulated reflectivity curves.

Figure 2 illustrates another example of interest: vastly different TE and TM measured spectroscopic reflectivity curves, for the same structure, are superimposed on corresponding simulated reflectivity curves. The simulated structures for each set of polarization are superimposed on top of

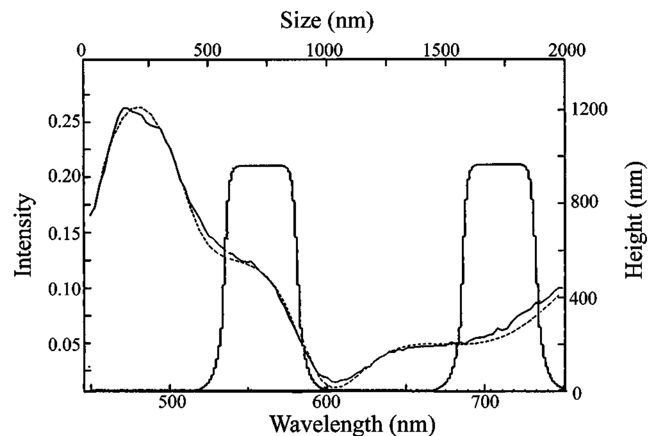

FIG. 1. Two sets of plots are shown in the same figure. One plot, using the left and bottom axes, show reflected light intensity vs wavelength, for both the experimental data (smooth curve) and simulated result (dotted curve). The other plot, using right and top axes, show the modeled photoresist profile used to generate the dotted intensity vs wavelength curve. From comparing the modeled intensity vs wavelength curve to the measured curve, the following measurements were obtained: Line height is 937 nm; linewidth at the bottom, midpoint, and top of the line profile are: 561, 328, and 231 nm, respectively.

[a)]Previously with: IBM Microelectronics, Essex Junction, VT 05452.
[b)]Electronic mail: dccole@bu.edu

 © 2002 American Institute of Physics
Downloaded 09 Jul 2002 to 128.197.27.175. Redistribution subject to AIP license or copyright, see http://ojps.aip.org/aplo/aplcr.jsp

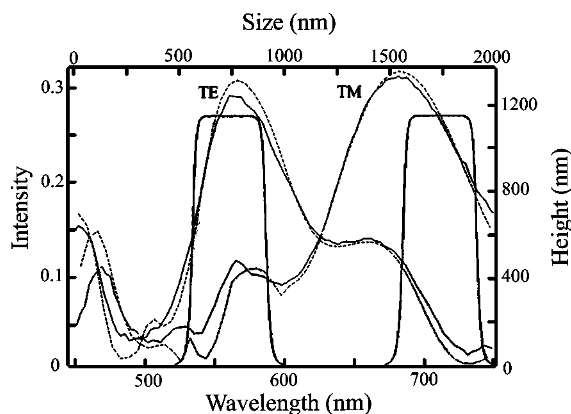

FIG. 2. TOK photoresist structure of norminal 500 nm lines and 1000 nm periodicity. TE and TM polarization reflectivity measurements (solid curves) are shown, along with their corresponding simulated reflectivity curves. For each curve, a separate physical structure was deduced. These two physical structure predictions are superimposed on top of each other here and are virtually indistinguishable from each other, at all points along the profile, including the rounded top and foot of the lines.

each other and are virtually indistinguishable.

Such modeled profiles have been generated in the past using a rather computationally intensive approach involving optimizing the number and sizes of a large number of ‘‘slabs’’ of photoresist to yield a reflectivity versus wavelength curve that most closely match the intensity data. This approach was originally pursued by two of us in microelectronics;[2] other researchers have also made investigations in scatterometry along these lines, or via matching precalculated libraries of shapes.[3–5] However, we have since completely revised and reformulated such approaches to enable a far more computationally efficient and robust algorithmic approach.[1] Indeed, this recently reported work extends 2D work by making use of a ‘‘single combined integral equation,’’ solved by the use of dyadic Green’s functions so that the microelectronic structure can be treated as a localized object embedded in a layered medium. By following this new approach, very fast and accurate 2D and 3D structures can be deduced, including contact holes and entire memory cell dimensions.

In this formulation, the electric and magnetic fields in each layered homogeneous region of a microelectronic structure are expressed in terms of a single, effective electric current density $\mathbf{J}_{\mathrm{eff}}$ flowing on the surface S of this region according to the following formulation:

$$\mathbf{E}(\mathbf{r},\omega)=j\omega\mathbf{A}(\mathbf{r},\omega)-\nabla\Phi(\mathbf{r},\omega),$$

$$\mathbf{H}(\mathbf{r},\omega)=\frac{1}{\mu_0}\nabla\times\mathbf{A}(\mathbf{r},\omega),$$

where ω indicates the Fourier frequency component of the indicated field. The vector and scalar potentials of $\mathbf{A}$ and Φ are in turn expressed in terms of a surface integral over the boundary of the medium, where the integrand involves a scalar Green’s function and the single effective current density field $\mathbf{J}_{\mathrm{eff}}(\mathbf{x},\omega)$.[1]

To demonstrate the flexible, yet powerfully predictive capability of this approach, measurements of photoresist profiles were taken by the far more standard metrology methods of SEM, as shown in Fig. 3, and AFM, as shown in Fig. 4.

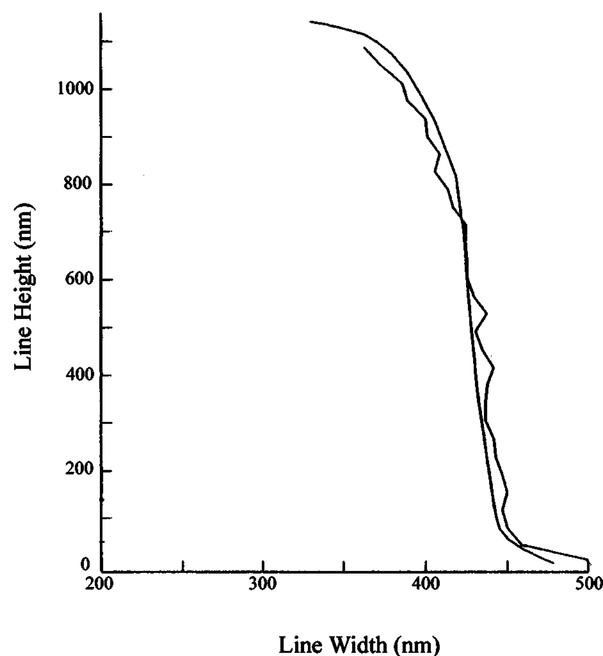

FIG. 3. Ragged curve represents data taken by SEM; the other curve is one taken using the electromagnetic scatterometry method discussed here. The horizontal axis represents the total width, at each height (y axis), for the photoresist profile.

Figure 3 represents the total photoresist width versus each height in the line profile; thus the average difference in measurement, per edge, would be half that shown. As can be seen, despite a profoundly nonlinear edge profile, the agreement is extremely close. We calculated an average slope difference of only about 1% between the two methods. Similarly, Fig. 4 shows a very close agreement in edge profile, despite the presence of an indented foot at the bottom and a slight T shape at the top.

An important distinction that needs to be noted here is that SEM and AFM methods are often destructive. Moreover, they require special laboratory setups not available in standard manufacturing semiconductor lines. Indeed, to ensure an accurate SEM measurement in Fig. 3, the wafer was cleaved so that the cross section could be scanned. The act of

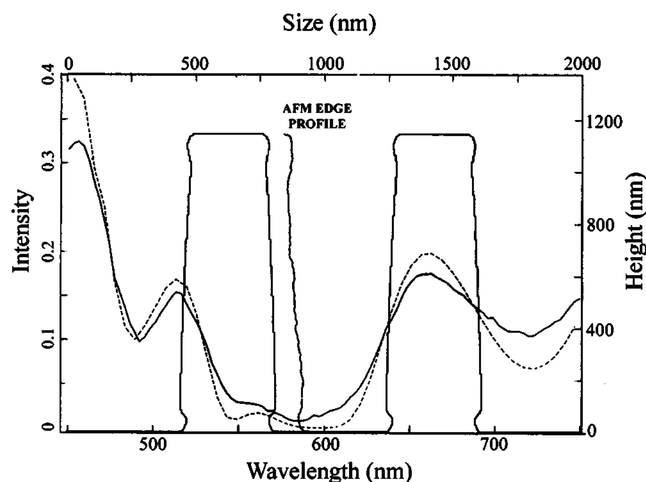

FIG. 4. One sidewall of one of the structures above was measured using AFM, as indicated, while the two full resist line profiles were computed from the light intensity scattering data. This AFM curve was displaced to the right to show how closely the detailed side profiles correspond.

Downloaded 09 Jul 2002 to 128.197.27.175. Redistribution subject to AIP license or copyright, see http://ojps.aip.org/aplo/aplcr.jsp

cleaving, calibrating, and measuring all require precise, careful, labor intensive steps. The present electromagnetic scatterometry method does not have these limitations. Moreover, with the accuracy and speed in the newly developed algorithmic approach in Ref. 1, 3D *in situ* measurements are becoming practical realities.

It is interesting to note why this electromagnetic scatterometry method is so accurate. The results are precisely opposite to what most technologists expect considering that the incident wavelength is considerably larger than the nanoscale profile features. Part of the explanation is that optical measurements are conventionally treated in the geometrical optical regime. A typical criterion for imaging in this regime is the Rayleigh resolution criteria,[6] which relates the approximate smallest geometrical spacing between objects to the wavelength of light used in the optical *imaging* of these objects. However, this resolution criterion does not apply to the scatterometry method, which does not entail optical imaging. Although a microscope setup is being used, the settings are not that for conventional geometrical imaging, but rather are set for achieving the detection of scattered light, for each polarization, at all wavelengths of reflected light. Thus, the entire diffraction theory of light propagation is taken into account, as fully embodied by all of Maxwell's equations in classical electromagnetic theory.[6,7] The signals of intensity versus wavelength in Figs. 1–4 have little bearing on a geometrical image of the structure. However, by properly taking into account the scattering of electromagnetic radiation off these nanoscale structures, detailed information on the structural nature can be obtained.

We conclude with the following observation. Since about 1990, the technology of phase shift masks and subresolution serif features has become a proven manufacturable means for printing photoresist structures with critical dimensions smaller than the exposure wavelength. The ''trick'' to achieving this was to not only recognize, but to take advantage of the fact that the optical mask can be engineered to be significantly different in structure from the intended printed photoresist shapes. This can be achieved only by moving away from the limitations of conventional geometrical ray optics so as to make full use of the diffraction theory of light when imaging and exposing photoresist.[8,9] In this letter, we see that provided the full electromagnetic scattering analysis is taken into account, detailed characterization of structures much smaller than the incident wavelength can be accurately achieved.

[1] M. Yeung and E. Barouch, Proc. SPIE **4344**, 484 (2001).
[2] D. P. Paul and E. W. Conrad, U.S. Patent No. 5,963,329 (listed at www.uspto.gov) pp. 1–24 (1999).
[3] J. Allgair, D. C. Benoit, R. R. Hershey, L. C. Litt, I. S. Abdulhalim, B. Braymer, M. Faeyrman, J. C. Robinson, U. K. Whitney, Y. Xu, P. Zalicki, and J. L. Seligson, Proc. SPIE **3998**, 125 (2000).
[4] X. Niu, N. Jakatdar, J. Bao, and C. J. Spanos, IEEE Trans. Semicond. Manuf. **14**, 97 (2001).
[5] H.-T. Huang, W. Kong, and F. L. Terry, Jr., Appl. Phys. Lett. **78**, 3983 (2001).
[6] M. Born and E. Wolf, *Principles of Optics*, 6th ed. (Cambridge University Press, Cambridge, UK, 1980).
[7] J. D. Jackson, *Classical Electrodynamics*, 3rd ed. (Wiley, New York, 1998).
[8] D. C. Cole, E. Barouch, U. Hollerbach, and S. A. Orszag, Jpn. J. Appl. Phys., Part 1 **31**, 4110 (1992).
[9] D. C. Cole, E. Barouch, E. W. Conrad, and M. Yeung, Proc. IEEE **89**, 1194 (2001).

Downloaded 09 Jul 2002 to 128.197.27.175. Redistribution subject to AIP license or copyright, see http://ojps.aip.org/aplo/aplcr.jsp